Supplementary Material: Use of marginal distributions constrained optimization (MADCO) for accelerated 2D MRI relaxometry and diffusometry

Dan Benjamini*, Peter J. Basser

Quantitative Imaging and Tissue Sciences, NICHD, National Institutes of Health, Bethesda, MD 20892, USA

1. PVP phantom: Ground truth and estimations from 1D experiments

Imaging the phantom allowed to separately analyze each of the (T_1, D) samples by selecting 3 regions of interest (ROI). The single peak 1D distributions obtained from separately analyzing these ROIs using data from 1D experiments were then averaged according to their relative spin density and taken as the 1D ground truth (Figs. 1A-B, empty red circles). The marginal T_1 and D distributions from a ROI that included all 3 (T_1, D) samples using 1D experiments is shown in Figs. 1A and B, respectively (full blue circles). These 1D estimations were used to constrain the 2D D-T_1 distribution reconstruction, resulting in a stabilization and acceleration of the process.

2. Conventional approach used for 2D reconstruction of D-T_1 spectrum

Reconstruction using the conventional experimental design at two representative data subsamples – 64, 157 – resulted in the 2D D-T_1 distributions shown in Fig. 2. Visually compared with the ground truth, the estimated results in Fig. 2 are highly inaccurate, both for the 2D and 1D projections.

*Corresponding author. Phone: +1-301-435-3868
Email address: dan.benjamini@nih.gov (Dan Benjamini)

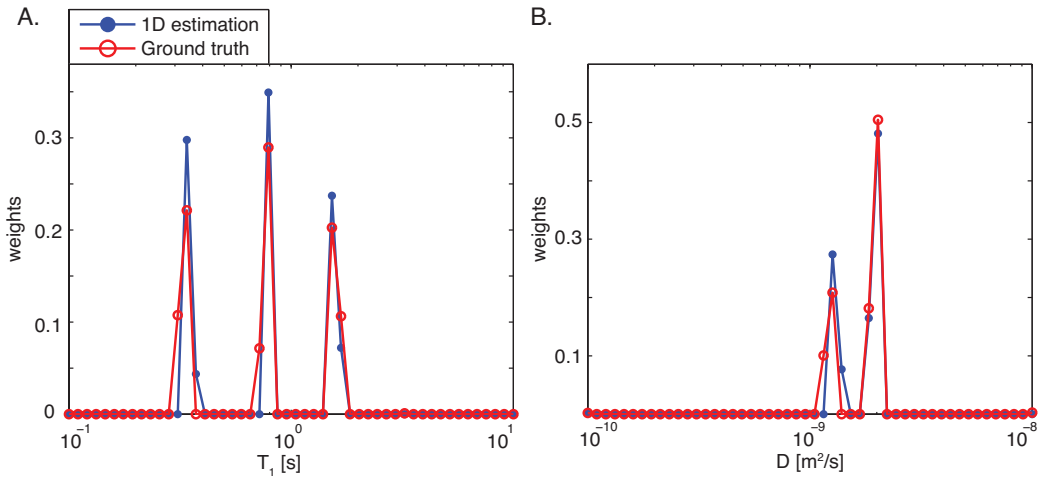

Figure 1: Comparison between ground truth (empty red circles) and estimations from 1D experiments (full blue circles). (A) Marginal T_1 and (B) Marginal D distributions, obtained from 1D acquisitions.

3. PVP phantom: Accuracy of the 2D distribution derived parameters

The accuracy of the estimated parameters, D, T_1, and the height of each peak, F, in the obtained 2D distributions, was determined by computing their normalized root mean square error (*nrmse*), ϵ, relative to the ground truth values (Table 1), which is defined as

$$\epsilon = \frac{\sqrt{\langle(\text{Estimated value} - \text{True value})^2\rangle}}{\text{True value}} \times 100, \tag{1}$$

where $\langle\cdots\rangle$ represents the geometrical mean. In terms of parameters accuracy, MADCO outperformed the conventional method in almost every instance, while consistently keeping the *nrmse* well-below 10%.

The *nrmse* values of single parameters from the distribution may be misleading – for example, the *nrmse* associated with the first two peaks in the spectrum obtained by using the conventional method with 64 acquisitions points to reasonable accuracy (Table 1) – while examination of the actual 2D spectrum (Fig. 2A) clearly shows that these peaks are not even resolved.

The actual estimated parameters, gm$D$, gmT_1, and the height of each peak, F, were determined by averaging over sections in the 2D distributions that correspond to the 3 distinct peaks. The partition between the peaks was

Table 1: Accuracy of the estimated 2D distribution derived parameters for the MADCO and conventional methods at different number of acquisitions. The *nrmse* [%] of the gmT_1, gm$D$, and F estimates of each peak relative to the ground truth values are expressed as ϵ_{T_1}, ϵ_D, and ϵ_F, respectively.

Peak		64 Acq. MADCO/Conv.	157 Acq. MADCO/Conv.	1480 Acq. MADCO/Conv.
1	ϵ_{T_1}	3.7 / 7.6	0.4 / 4.3	0.7 / 5.9
	ϵ_D	8.8 / 1.5	0.8 / 2.0	2.9 / 4.3
	ϵ_F	4.8 / 1.1	8.4 / 6.1	8.6 / 1.7
2	ϵ_{T_1}	0.5 / 6.0	1.6 / 8.7	1.4 / 18
	ϵ_D	9.1 / 6.8	6.2 / 2.7	3.6 / 14
	ϵ_F	0.1 / 25	8.9 / 31	6.1 / 63
3	ϵ_{T_1}	12 / 9.2	2.9 / 12	1.1 / 18
	ϵ_D	13 / 29	2.3 / 11	2.3 / 14
	ϵ_F	5.4 / 30	5.4 / 43	2.9 / 75

determined according to the ground truth distribution (Fig. 1 in the main paper): (1) $100 \leq T_1 \leq 494$ ms (2) $543 \leq T_1 \leq 954$ ms (3) $1048 \leq T_1 \leq 10000$ ms. Note that the entire range of diffusivities was included in each peak. The resulting parameters are detailed in Table 2.

Table 2: Accuracy of the estimated 2D distribution derived parameters for the MADCO and conventional methods at different number of acquisitions.

		Truth	64 Acq.		157 Acq.		1480 Acq.	
			MADCO	Conv.	MADCO	Conv.	MADCO	Conv.
Peak 1	gmT_1 [ms]	293	304	316	292	306	291	311
	gm$D$ [μm^2/ms]	2.26	2.06	2.23	2.25	2.22	2.20	2.17
	F	0.35	0.33	0.34	0.32	0.33	0.32	0.34
Peak 2	gmT_1 [ms]	782	778	735	769	714	771	641
	gm$D$ [μm^2/ms]	1.99	1.81	1.86	1.87	1.94	1.92	2.27
	F	0.35	0.35	0.26	0.38	0.24	0.37	0.13
Peak 3	gmT_1 [ms]	1596	1785	1449	1643	1406	1613	1307
	gm$D$ [μm^2/ms]	1.24	1.39	1.36	1.26	1.37	1.26	1.41
	F	0.30	0.32	0.40	0.30	0.43	0.31	0.53

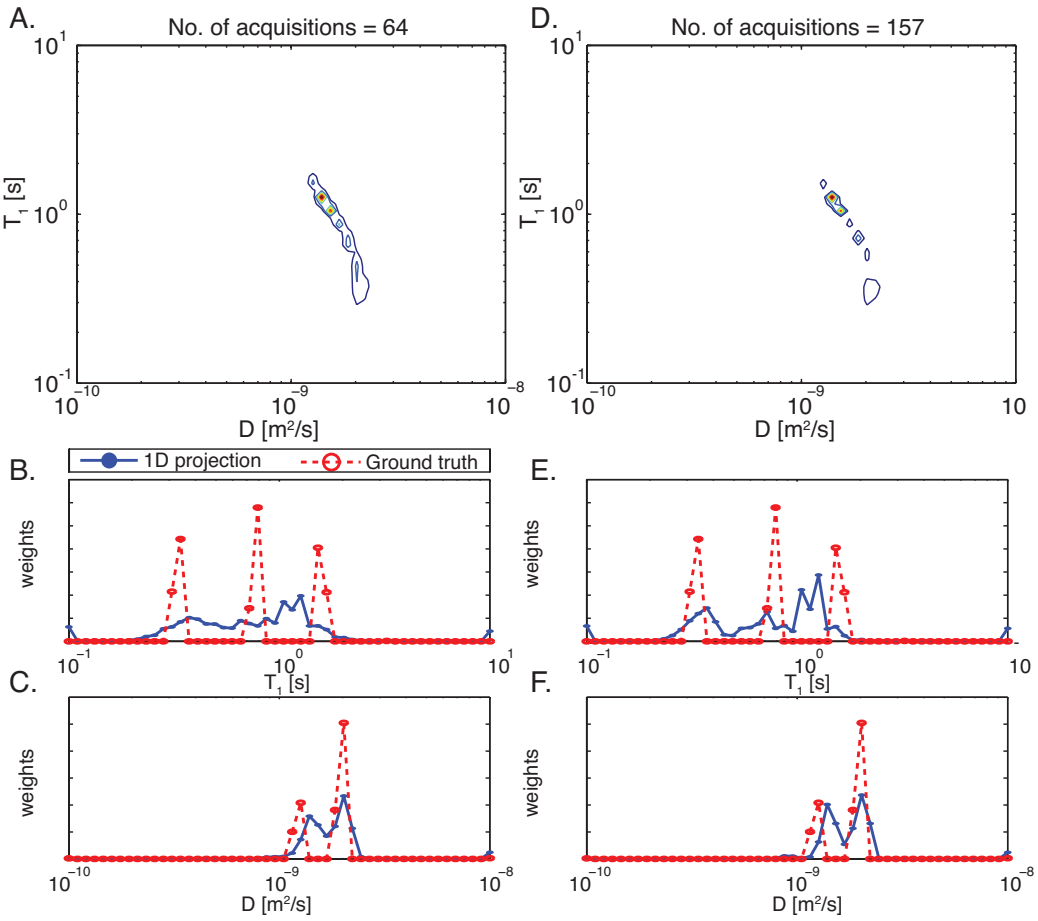

Figure 2: Reconstruction with the unconstrained conventional method. Two data subsamples resulted in the 2D D-T_1 distributions in A and B. Below are the 1D projections (blue circles) overlaid with the ground truth 1D distributions (red circles).